Fronthaul Network Architecture and Design For Optically Powered Passive Optical Networks

Egemen Erbayat[1], Shrinivas Petale[1], Shih-Chun Lin[2], Motoharu Matsuura[3], Hiroshi Hasegawa[4], Suresh Subramaniam[1]
[1]*The George Washington University*, [2]*North Carolina State University*, [3]*University of Electro-Communications*, [4]*Nagoya University*
[1]{*erbayat, srpetale, suresh*}*@gwu.edu*, [2]*slin23@ncsu.edu*, , [3]*m.matsuura@uec.ac.jp*, [4]*hasegawa@nuee.nagoya-u.ac.jp*

***Abstract*—With the evolution of modern telecommunications, the fronthaul network has become an indispensable component of the infrastructure, particularly in the context of Cloud Radio Access Networks. Nevertheless, fronthaul networks still face significant challenges such as power outages, particularly when a disaster, like an earthquake or severe weather event, occurs. Damage to power supply facilities may cause operational failures while communication is one of the most crucial needs in the disaster area to make rescue operations more effective. Specialized fibers that can deliver electrical power can help mitigate this problem. However, power losses may be extremely large over distances and there is no flexibility after the installation of the fibers. The network topology design that reduces capital and operational costs while satisfying power constraints is an important problem. In this paper, we focus on network topology design in an urban area by taking into account both fiber and power costs. We then propose integer linear programming and fast algorithms based on methods for single-facility location problems. The results demonstrate that multiple approaches help to achieve the optimal design, with our proposed method standing out due to its efficiency in finding feasible solutions, scalability, and ≈656x reduction in execution time.**

***Index Terms*—Power over Fiber, Integer Linear Programming, Fronthaul Networks, Optimization, Weiszfeld Procedure**

I. Introduction

The demand for higher data rates, lower latency, and increased reliability has escalated dramatically with the evolution towards 5G/6G technologies. To meet these requirements, Cloud Radio Access Networks (C-RANs) have emerged as a vital architecture [1]. In C-RAN, baseband processing is centralized in a data center. This enables more efficient resource utilization and dynamic allocation, which is crucial for the advanced features of 5G/6G networks. However, the primary challenge in 5G/6G deployment is the need for high network density. To support a massive number of devices and connections per square kilometer, reliable networks must be designed with unprecedented density. To address these demands, remotely powered fronthaul networks are considered a promising solution.

In an urban fronthaul network, a reliable power supply is essential to maintain uninterrupted communication, and any damage to power supply facilities can lead to operational failures. Typically, these networks depend on electrical power grid connections, making them susceptible to power outages. In the event of a significant disaster, a huge area can experience power outages, regardless of the city's large resources, as seen in scenarios like earthquakes in Los Angeles [2] and storms in New York [3]. In a typical fronthaul network, an Edge Cloud (EC) and the Remote Radio Heads (RRHs) are connected via optical fibers for data transmission and separate units are dedicated to power transmissions [4]. With the introduction of the new technology, optical fibers enabled with power-over-fiber (PWoF) technology can carry both transmission data and power at the same time [5], [6]. Such fibers can help avoid separate power units. This could not only provide an economical solution for powering RRHs in urban areas by reducing high power facility costs, but also enhance network resilience in the event of power outages caused by disasters in city centers providing microgrids. One of the traditional methods in the disaster area to recover power supply quickly is providing portable and mobile power supplies like generators, but typically, they only serve the buildings attached to those generators [7], [8]. Microgrids can be established by deploying PWoF technology and the required power for RRHs can be supplied over those fibers from a single generator at EC. This design makes power available for larger areas at low capital expenditures (CapEx) by distributing backup power generated at specific locations instead of having a backup source at each RRH location. In order to reduce CapEx, a special splitter can be used to connect the RRHs and EC. However, the power transmitted through the PWoF may experience degradation based on the length of the fiber. Therefore, the placement of the splitter plays a crucial role in ensuring a robust network architecture while keeping the CapEx to a minimum. It is important to plan the network carefully, as any post-deployment modifications can result in high CapEx and resource wastage. The distance between the splitter and RRHs and EC determines the inventory required for optical fiber and power generation. Longer distances can lead to higher CapEx and operating expenditure (OpEx), including power costs. In addition, the fiber technology used to connect the EC to the splitter and then the splitter to the RRHs may have different requirements, resulting in different CapEx and OpEx. Therefore, the location that has higher CapEx may have less OpEx and total cost, and vice versa.

In this paper, we propose various approaches to solve the problem of optimal splitter position while satisfying all the power and loss constraints and minimizing the incurred cost. We first discuss integer linear programming (ILP), convex optimization, and an exhaustive search algorithm. Then, we leverage the similarity between our problem and the single facility location problem [9] and propose a new algorithm to enhance single-facility location solutions. We apply those algorithms to various topologies with various parameters and show that the performance can be improved dramatically without causing high execution time.

The rest of the paper is organized as follows. We present the network model and the details of the fibers we choose in Section II. In Section III, we describe the problem. Then, we formulate an ILP and present algorithms to minimize the cost. Finally, we compare results and validate our heuristic algorithms in Section IV, and then we present our conclusions in the last section.

II. Network Model

We consider an optically-powered passive optical network (PON) architecture that has RRHs connected to an EC through the splitter. The system model used in our work is shown in Fig. 1. This paper considers the case of a single EC and splitter. Our future research will explore scenarios involving multiple ECs and splitters.

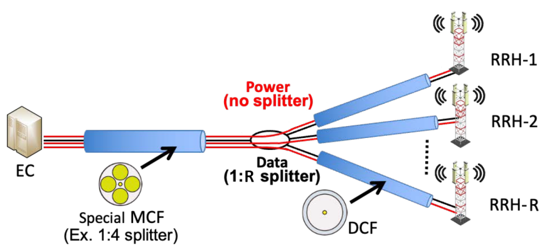

Fig. 1: The fronthaul PWoF network model, EC: edge cloud, RRH: remote radio head, MCF: multi-core fiber, DCF: double-clad fiber.

The optical splitter is used to enable a signal on an optical fiber to be distributed among two or more fibers. The splitter's number of ports is greater than or equal to the number of cores and supported RRHs. Before the splitter, we prefer multi-core fibers (MCFs) to reduce the number of fibers. MCF consists of a single-mode (SM) core for data transmission and multi-mode (MM) cores that surround the SM core for optical power transmission. We assume seven core multicore fiber to support at most six RRHs [10].[1] After the splitter, double-clad fibers (DCFs) are preferred because DCFs provide higher electric power[2] than conventional technologies [11]. Data is transmitted in the SM core and power is transmitted in the inner cladding of each DCF. We also consider that the couplers of current DCF technology limit the maximum power per DCF from the splitter [12]. We assume that fibers have exponential power losses. We consider a square network map M with grid dimensions $n \times n$ and with each side being k kilometers long. This map consists of n^2 grid coordinates evenly spaced at intervals of k/n kilometers. Locations of the EC, the splitter, and the RRHs are chosen among these coordinates. We employ Manhattan distance as our distance metric. We consider a grid layout and Manhattan distance because deploying optical fibers under the streets in city centers like New York or Los Angeles is the preferred way than placing them under the buildings [13].

[1]The optimization can run for any multicore fiber geometry and fiber bundle.
[2]Note that DCF fibers carry optical power which is converted to electrical power at the RRH. We call it electrical power or simply power to avoid confusion with signal optical power.

III. Problem Description and Solutions

In this section, we first explain the problem formulation. Later, we present various solution approaches, including ILP, exhaustive search, and heuristic algorithms. In our network design problem, we define several key parameters and notations: We denote the coordinates of the EC, the i^{th} RRH, and the splitter as (e_x, e_y), (r_{i_x}, r_{i_y}), and (s_x, s_y), respectively. The set of RRH positions and the number of RRHs are represented as R and $|R|$, respectively. We also define d^{es} as the distance between the EC and the splitter, and d^{sr_i} as the distance between the splitter and the i^{th} RRH, both expressed as non-negative integers. For cost calculations, we introduce ζ^{mm}, ζ^{sm}, and ζ^{dcf} as the cost per unit length for MM core [14], SM core [14], and DCF [11], respectively. Additionally, γ^{mm} and γ^{dcf} represent the power loss per unit length for MM core and DCF.

In addition, we define the power provided by EC and the maximum power that can be provided by EC as P^e and P^e_{max}, respectively. The maximum power that can be supplied by the splitter for each DCF is $P^{\mathrm{dcf}}_{\mathrm{max}}$. The minimum power required at the i^{th} RRH is P^{r_i}. β denotes the power generation cost per watt at the EC and t is operating time. Furthermore, we use f to indicate the cost of fiber used, and p for the power cost. Table I summarizes the notations used in the paper.

The formulation, which is based on the assumption that the positions of the EC and RRHs remain fixed, and our design focus solely on determining the optimal placement of the splitter, as given in (1)-(10). Therefore, the only decision variable is the splitter position and it must be between the EC and RRHs, as shown in (2) and (3) As a constraint, each DCF must provide the required power after power loss and the total power provided by the EC must be less than the maximum power the EC can provide as shown in (4), (5) and (6). To maintain simplicity, we exclude constant costs such as installation expenses, as these remain consistent regardless of the splitter's position within the network. In (7), the total cost for all fiber types is calculated as the sum of the product of each fiber type's length and its respective cost per unit length. Additionally, it is important to note that fiber and power costs can vary significantly depending on geographic location. To account for this variability, we employ relative costs and introduce the parameter β to adjust the weightings as shown in (8). This approach allows our algorithm to adapt and perform effectively across diverse scenarios.

Objective: Minimize the total cost, represented as the sum of the fiber cost and the power cost over time.

$$minimize_{s_x,s_y} : f + p \times t \tag{1}$$

Variables:

$$\min\{e_x, r_{i_x}, \forall r_{i_x} \in R\} \le s_x \le \max\{e_x, r_{i_x}, \forall r_{i_x} \in R\} \tag{2}$$

$$\min\{e_y, r_{i_y}, \forall r_{i_y} \in R\} \le s_y \le \max\{e_y, r_{i_y}, \forall r_{i_y} \in R\} \tag{3}$$

Constraints:

$$\forall r_i \in R : 10^{\frac{d^{\mathrm{sr_i}}\gamma^{\mathrm{dcf}}}{10}} P^{r_i} \le P^{\mathrm{dcf}}_{\mathrm{max}} \tag{4}$$

$$\sum_{i=1}^{|R|} \left(10^{\left(\frac{d^{\mathrm{es}}\gamma^{\mathrm{mm}} + d^{\mathrm{sr_i}}\gamma^{\mathrm{dcf}}}{10}\right)} P^{r_i} \right) = P^e \tag{5}$$

$$P^e \leq P^e_{\max} \tag{6}$$

$$f = d^{\text{es}}(\zeta^{\text{sm}} + |R|\zeta^{\text{mm}}) + \sum_{i=1}^{|R|} d^{\text{sr}_i}\zeta^{\text{dcf}} \tag{7}$$

$$p = \beta P^e \tag{8}$$

Manhattan Distance:

$$d^{es} = |e_x - s_x| + |e_y - s_y| \tag{9}$$

$$d^{sr_i} = |s_x - r_{i_x}| + |s_y - r_{i_y}| \tag{10}$$

TABLE I: Network notation.

Notation	Description
$e = (e_x, e_y)$	Position of the EC
$r_i = (r_{i_x}, r_{i_y})$	Position of the i^{th} RRH
$s = (s_x, s_y)$	Position of the splitter
R	The set of RRHs' positions
$\|R\|$	The number of RRHs
S	The set of positions for the candidate splitters
$s_i = (s_{i_x}, s_{i_y})$	Position of the i^{th} candidate splitter
d^{es}	The distance from the EC to the splitter
d^{sr_i}	The distance between the splitter and the i^{th} RRH
ζ^{mm}, ζ^{sm}, ζ^{dcf}	The cost per unit length for multi-mode core (MM), single-mode core (SM), and double-clad fiber (DCF), respectively
γ^{mm}, γ^{dcf}	The power loss per unit length for MM and DCF
P^e	Power provided by the EC
$P^e_{\max}$	Maximum power can be provided by the EC
$P^{\text{dcf}}_{\max}$	The maximum power that can be supplied by the splitter for each DCF
P^{r_i}	The power requirement at i^{th} RRH
β	The power generation cost per watt at the EC
t	Operating Time
f	Fiber Cost
p	Power Cost
n	Map Size
M	The $n \times n$ map
k	The real side length of the map in kilometers

A. *Feasibility of Given Topology*

The maximum distance between the splitter and each RRH is restricted by (4). In essence, each RRH defines a coverage area, and the optimal placement of the splitter must align with the intersection of these areas. When the RRHs are widely spaced apart, finding a feasible solution becomes increasingly challenging. The shape of these coverage areas resembles diamonds due to the Manhattan distance metric, with the radius depending on the power requirement and γ^{dcf}. A lower power requirement results in a larger coverage radius. Therefore, the feasibility problem involves finding an enclosing weighted diamond where the weights are determined by power requirements. For example, there must be at most a 3 dB loss for a $10W$ requirement, whereas a 6 dB loss is acceptable for a $5W$ requirement if $P^{\text{dcf}}_{\max}$ is 20W. The relationship can be seen in Figure 2. When $\gamma^{\text{dcf}} = 1.5$ dB/km, R_0 must be at most 2 km to find a feasible solution.

B. *ILP Formulation*

The decision variable in this scenario is the placement of the splitter. However, using the splitter location as a decision variable results in non-linear constraints and objectives due to the Manhattan distance metric. To obtain a linear formulation, we consider every grid point of the map to be a potential splitter location and the decision variables indicate which one of these points is selected to be the splitter location. The set of candidate splitter positions is represented as S where (s_{i_x}, s_{i_y}) is the position of the i^{th} candidate splitter. Then, distance values become constant values and we do not have any non-linearity. The ILP is thus formulated as follows:

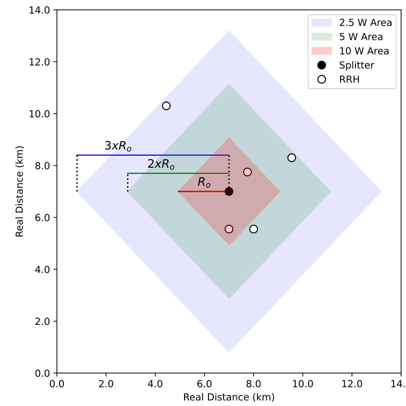

Fig. 2: Splitter coverage areas for different power requirements.

Candidate Splitter Positions:

$$min\{e_x, r_{i_x}, \forall r_{i_x} \in R\} \leq s_{j_x}, \forall s_{j_x} \in S \leq max\{e_x, r_{i_x}, \forall r_{i_x} \in R\} \tag{11}$$

$$min\{e_y, r_{i_y}, \forall r_{i_y} \in R\} \leq s_{j_y}, \forall s_{j_y} \in S \leq max\{e_y, r_{i_y}, \forall r_{i_y} \in R\} \tag{12}$$

Variables:

$$S_i = \begin{cases} 1, & \text{if the } i^{th} \text{ splitter position is selected,} \\ 0, & \text{otherwise} \end{cases} \tag{13}$$

Splitter Constraint:

$$\sum_{i \in S} S_i = 1 \tag{14}$$

C. *Exhaustive Search*

To find the exact solution, which is the global minimum for the objective function, we have to consider all possible locations for the splitter. We define an exhaustive search algorithm to check every possible splitter location. It takes the vector V consisting of parameter values for $\beta, \zeta, \gamma, \cdots$, a $(|R|+1) \times 2$ matrix P which represents the positions of the RRHs and EC. $(P_{i,1}, P_{i,2})$ represents coordinates of the i^{th} element. Then, the algorithm gives the optimal splitter position S_{opt} and the corresponding cost C. The optimal splitter position can be obtained by the exhaustive search algorithm; however the time complexity of the exhaustive search algorithm is $O(n^2|R|)$. The time complexity is increased dramatically with the increase of map size. Therefore, we look for heuristic algorithms.

D. *Convex Optimization*

To avoid non-linear constraints and objective function using Manhattan distance, we have to design a complex ILP model with a large number of variables. Therefore, we also use convex optimization (CO) to cope with the large number of variables. Using convex optimization, we are able to use the splitter position as a decision variable. However, CO is focused on continuous optimization. Continuous optimization involves a tradeoff between advantages and disadvantages. The time complexity is independent of the map size, but it gives non-discrete results. We use CO followed by rounding to get a solution for the splitter position with discrete coordinates.

Algorithm 1: Exhaustive search.

```
Input: M, V, P
Output: S_opt, C
Initialize:
Optimal Cost ← ∞,
S_opt ← (0, 0)
for each (i, j) coordinates in map M do
  if The power constraints are satisfied by the coordinates (i, j) then
    Place the splitter on the position (i, j) and calculate the cost.
    Compare its cost with the last calculated optimal cost.
    If the cost is less than the optimal cost, update the optimal cost and optimal splitter position S_opt
  end if
end for
Save S_opt
```

E. Heuristic Algorithms

We use the same notation as in exhaustive search for the heuristic algorithms. Also, we define an $R \times 1$ weight vector W, which corresponds to a weight for each RRH. We are inspired by (4) while deciding the weights. We assign $w_i = \gamma^{\text{dcf}}/(10\log(P^{\text{dcf}}_{\max}/P^{r_i}))$ for RRHs as weights.

1) **Weighted Weiszfeld Procedure (WWP)**
Weiszfeld Procedure [15] is a mathematical technique used for finding the geometric median (GM) of a set of points in Euclidean space. It offers an iterative approach to locate the point that minimizes the sum of distances to all other points. We use a weighted version of that procedure to consider point significance.

$$(\bar{S}_{opt_x}, \bar{S}_{opt_y}) = \underset{(x,y)}{\arg\min} \sum_{i=1}^{R} w_i \sqrt{(x - P_{i,1})^2 + (y - P_{i,2})^2} \tag{15}$$

2) **Minimax Location Problem (MLP)**
The Minimax Location Problem [9] is a type of optimization problem that deals with the selection of locations for facilities to minimize the maximum possible cost or distance between the facilities and the demand points. In our case, the minimization problem becomes:

$$\min_{s=(s_x,s_y)} \max_{1\leq n\leq |R|} w_i d^{sr_i}. \tag{16}$$

Note that the objective has similarities with the problem in Section III-A. The optimal solution of the given minimax problem is the center of the minimum enclosing diamond, and the objective value is its radius. In this method, we use that center as S_{opt}. Both WWP and MLP are for continuous optimization. There is the same tradeoff we have for CO. We are expecting a non-discrete solution within an execution time that is independent of the map size. We again use rounding to make solutions dicrete.

3) **Local Optimum**
We use this algorithm to improve the results obtained by WWP, MLP, and CO. First, we find a point using those algorithms and then put that point in the local optimum algorithm (LO) to get better results. The local optimum algorithm checks whether there is a neighbor with a lower cost or not. If yes, the optimal point is moved and if not, return the optimal point.

Algorithm 2: Local optimum.

```
Input: M, V, P, S_opt, C
Output: S_opt, C
while true do
  Check four 4-neighbor coordinates' costs and compare them with C.
  Find the neighbor with the lowest cost, and move the corresponding position if it meets the power constraints and update S_opt.
  if the position stays the same then
    break
  end if
end while
Save S_opt
```

We need an initial S_{opt} for LO and it is obtained by WWP, MLP, or CO. These algorithms are denoted WWP+LO, MLP+LO and CO+LO, respectively.

IV. Simulation Results

We now present the outcome of extensive simulations to find the splitter position using the proposed approaches. The performance and complexity of our system are linked to these key variables: map size n and the number of RRHs $|R|$. To observe the effects of these parameters, we conducted our simulation 100 times for each combination of parameters using the constants $\zeta^{\text{mm}} = 1.5$ km^{-1}, $\zeta^{\text{sm}} = 1$ km^{-1}, $\zeta^{\text{dcf}} = 3$ km^{-1}, $\gamma^{\text{mm}} = 1$ dB/km, $\gamma^{\text{dcf}} = 1.46$ dB/km, $P^{e}_{max} = 500$ W, $P^{\text{dcf}}_{\max} = 20$ W, $\beta = 0.1\text{W}^{-1}$, $t = 10$ years, and $k = 4$ km; while ensuring a topology that has a feasible solution. The locations of RRHs and the EC are randomly chosen for every trial, with defined EC and RRH zones in place to avoid unrealistic topologies, see Figure (3a, 3b). Each device must remain within its defined zone.

Our analysis focuses on three key performance metrics – average execution time, ratio of finding feasible solutions out of 100 runs, and global optimal using exhaustive search for comparison because we know that an exhaustive search guarantees the optimal splitter location with the minimum cost by exploring every possible position. We use mean absolute percentage error (MAPE) for evaluation, (17). Note that while ILP consistently identifies an optimal position for each trial, we have chosen not to include ILP results due to the added complexity resulting from linearization which causes prohibitive execution time when applied to the single splitter case. However, it is important to note that ILP will play a crucial role in the cases of multiple ECs and/or splitters, which is part of our future research.

$$MAPE = \frac{1}{T}\sum_{i=1}^{T}\frac{|C_i - C_{ex,i}|}{C_{ex,i}} \times 100, \quad (17)$$

where C_i is the cost of the chosen algorithm at i^{th} trial, $C_{ex,i}$ is the cost of the exhaustive search algorithm at i^{th} trial, and T is the number of feasible solutions found by the chosen algorithm.

Initially, we focus on the effect of map size. We set $|R| = 5$ and $P^r = (10, 10, 10, 10, 10)$ [16] The map size has a huge impact on the performance of algorithms in two ways. First, the complexity grows with n^2. As seen in Table II, the execution time is increased for exhaustive search and LO enhancement. A change in map size does not affect the other three methods' execution time because they take the map as a continuous map. To investigate the other algorithms' performance, we collect the ratio of feasible solutions returned by those algorithms to the number of feasible solutions found by exhaustive search.

TABLE II: Map size versus execution time(ms).

	Map Size (M)				
Approach	30	100	300	500	1000
Exhaustive	104	923	7201	22108	79754
WWP	0.3	0.4	0.5	0.6	0.8
MLP	10.3	10.3	9.8	11.6	11.5
CO	117.4	113.1	137.5	128.3	117.8
WWP+LO	9	23.5	68.3	142.5	287.2
MLP+LO	14.4	22.6	40.4	65.9	98.5
CO+LO	118.9	115.7	141.8	131.6	121.4

TABLE III: Map size versus the ratio of infeasible solutions.

	Map Size (M)				
Approach	30	100	300	500	1000
WWP	59	54	52	62	71
MLP	0	0	0	0	0
CO	15	80	77	81	16
WWP+LO	29	35	36	46	47
MLP+LO	0	0	0	0	0
CO+LO	0	0	0	0	0

The MLP and CO algorithms are directly based on power requirements, whereas the WWP algorithm is based on minimum cost without considering power requirements. Therefore, we expect the MLP and CO algorithms to return feasible solutions, while the WWP algorithm may not, and LO enhancement helps the WWP algorithm to find a feasible solution. Our expectation is verified by Table III, except for CO. The reason behind that is rounding. CO finds a non-integer solution, and we have to round it. However, the optimal solution may be at the edge of one RRH coverage area and it may be out of that area after rounding. To deal with this issue, we can apply LO enhancement. We do not encounter this problem with MLP, despite it providing a non-integer solution. This is because MLP aims to find the minimum enclosing diamond, so rounding does not significantly affect the coverage.

When we look at Table IV, we can see that LO enhancement reduces the error for all three algorithms. It can be easily seen that CO+LO outperforms other algorithms. However, zero error does not mean that both exhaustive search and CO+LO find the same point as optimal. When there are more than one optimal

TABLE IV: Map size versus error.

	Map Size (M)				
Approach	30	100	300	500	1000
WWP	11.1	10.5	11.9	10.5	12.2
MLP	10.3	13.2	10.5	10.9	10
CO	0.808	0.215	0.147	0.033	0.039
WWP+LO	0.4	0.5	0.6	0.4	0.4
MLP+LO	1.6	2.3	0.9	0.6	0.8
CO+LO	0	0	0	0	0

points for a given topology, the optimal locations may be different. For example, an exhaustive search algorithm finds the optimal splitter position as $(240, 335)$ with the cost of 250.71 for the topology in Figure (3c). However, the other algorithms find that the optimal position is different than the exhaustive search, Figure (3d, 3e). $(243, 337)$ and $(243, 338)$ are the optimum locations given by CO and CO+LO, respectively. The convex optimization solution is at the edge, thus rounding gives an infeasible location. The calculated costs are exactly the same, while the optimal points obtained by exhaustive search and CO+LO are different.

TABLE V: Number of RRHs versus the ratio of infeasible solutions

	Number of RRHs ($|R|$)				
Approach	2	3	4	5	6
WWP	0	45	55	62	68
MLP	0	0	0	0	0
CO	25	53	73	81	87
WWP+LO	0	21	25	46	43
MLP+LO	0	0	0	0	0
CO+LO	0	0	0	0	0

TABLE VI: Number of RRHs versus error.

	Number of RRHs ($|R|$)				
Approach	2	3	4	5	6
WWP	17	12.7	12.9	10.5	10.4
MLP	16.1	14.4	12.2	10.9	7.9
CO	0.069	0.208	0.349	0.033	0.042
WWP+LO	0	0.2	0.2	0.4	0.4
MLP+LO	0	1.1	0.7	0.6	0.9
CO+LO	0	0	0	0	0

In addition to map size, the number of RRHs has an effect on the algorithms because MLP and WWP use RRH positions as optimization inputs and an increase in the number of RRHs means an increase in complexity. In Table V, the number of RRHs effects can be seen. An increase in the number of RRHs reduces the number of potential splitter locations, which causes higher infeasibility rates. For $|R| = 2$, WWP+LO and MLP+LO also give zero error as well as CO+LO. We have also conducted a sensitivity analysis of β, and have found that the optimal splitter location is not very sensitive to that parameter (though the cost would obviously differ). These results are not presented here for space reasons.

When we consider all cases, it can be easily seen that the CO+LO algorithm is superior to other algorithms. The most important aim in our case is getting a position with the lowest cost. CO+LO successfully enables us to get the optimal position. In addition, it has a significantly smaller execution time when compared to the exhaustive search method that gives optimal positions.

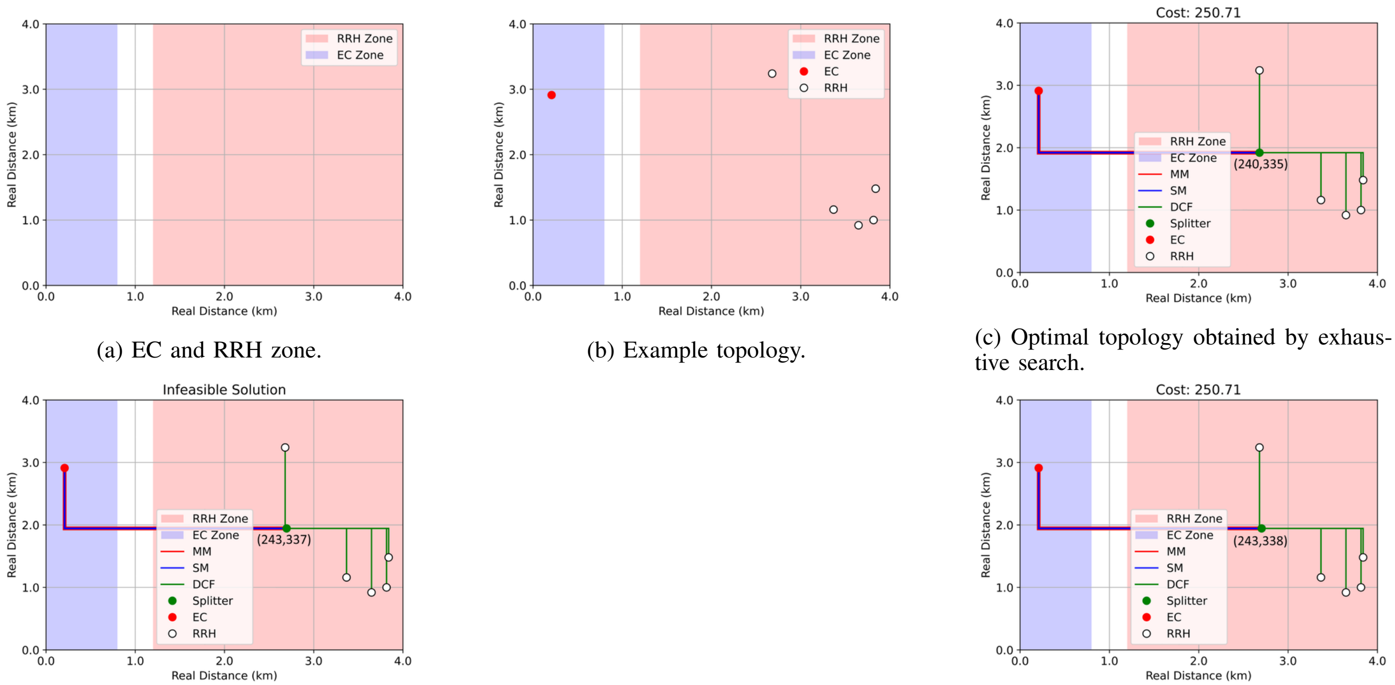

(a) EC and RRH zone.

(b) Example topology.

(c) Optimal topology obtained by exhaustive search.

(d) Optimal topology obtained by CO.

(e) Optimal topology obtained by CO+LO.

Fig. 3: Simulation results for an example topology for $n = 500$, $|R| = 5$.

V. Conclusion

In the era of advanced telecommunications, fronthaul networks are essential, particularly in C-RANs. Yet, power outages during disasters like earthquakes can disrupt critical communication. To address this challenge, we examined the use of power-delivering fibers. While promising, managing power losses over distances and installation flexibility remain concerns. Our study emphasizes cost-effective network topology design while respecting power limitations. In this paper, algorithms are investigated to attain the minimum sum of fiber and power costs in a simple case of a fronthaul network in an urban setting. Our results show the feasibility of optimal network designs, with our method standing out due to its efficiency, scalability, and a remarkable 656x reduction in execution time. Our initial focus was on demonstrating the applicability of such a design; future work will explore more complex networks, including multiple ECs and splitters that can serve many more RRHs and more general environments.

Acknowledgment

This work was supported in part by NSF grants CNS-1813617, CNS-2210343 and CNS-1818858.

References

[1] A. Checko, H. L. Christiansen, Y. Yan, L. Scolari, G. Kardaras, M. S. Berger, and L. Dittmann, "Cloud RAN for Mobile Networks—A Technology Overview," *IEEE Communications Surveys & Tutorials*, vol. 17, no. 1, pp. 405–426, 2015.

[2] X. Dong, M. Shinozuka, and S. Chang, "Utility Power Network Systems," in *Proceedings of 13th World Conference on Earthquake Engineering*, 2004.

[3] T. C. of New York, "A Stronger, More Resilient New York." Chapter 6: Utilities, June 11, 2013 2013. Accessed: October 31, 2023.

[4] C. Ranaweera, E. Wong, A. Nirmalathas, C. Jayasundara, and C. Lim, "5G C-RAN With Optical Fronthaul: An Analysis From a Deployment Perspective," *Journal of Lightwave Technology*, vol. 36, no. 11, pp. 2059–2068, 2018.

[5] M. Matsuura and J. Sato, "Bidirectional Radio-Over-Fiber Systems Using Double-Clad Fibers for Optically Powered Remote Antenna Units," *IEEE Photonics Journal*, vol. 7, no. 1, pp. 1–9, 2015.

[6] M. Matsuura, "Power-over-Fiber for Remote Antenna Units in 5G/6G Networks," in *2023 Opto-Electronics and Communications Conference (OECC)*, pp. 1–2, 2023.

[7] G. Davis, A. F. Snyder, and J. Mader, "The future of Distribution System Resiliency," in *2014 Clemson University Power Systems Conference*, pp. 1–8, 2014.

[8] J. Xia, F. Xu, and G. Huang, "Research on Power Grid Resilience and Power Supply Restoration during Disasters-A Review," in *Flood Impact Mitigation and Resilience Enhancement* (G. Huang, ed.), ch. 8, Rijeka: IntechOpen, 2020.

[9] E. Moradi and M. Bidkhori, *Single Facility Location Problem*, pp. 37–68. Heidelberg: Physica-Verlag HD, 2009.

[10] S. Petale, J. Zhao, and S. Subramaniam, "TRA: an efficient dynamic resource assignment algorithm for MCF-based SS-FONs," *J. Opt. Commun. Netw.*, vol. 14, pp. 511–523, Jul 2022.

[11] M. Matsuura, "Power-Over-Fiber Using Double-Clad Fibers," *Journal of Lightwave Technology*, vol. 40, no. 10, pp. 3187–3196, 2022.

[12] K. Murakami, H. Mamiya, and M. Matsuura, "Improvement of Power Transmission Efficiency in Power-over-Fiber Using a Double-Clad Fiber at 1550 nm," in *2022 27th OptoElectronics and Communications Conference (OECC) and 2022 International Conference on Photonics in Switching and Computing (PSC), Toyama, Japan, July 3-6, 2022*, pp. 1–3, IEEE, 2022.

[13] G. V. Arévalo, J. E. Sierra, R. C. Hincapié, and R. Gaudino, "A novel algorithm for PON optimal deployment over real city maps and large number of users," in *18th Italian National Conference on Photonic Technologies (Fotonica 2016)*, pp. 1–4, 2016.

[14] M. Klinkowski, P. Lechowicz, and K. Walkowiak, "Survey of resource allocation schemes and algorithms in spectrally-spatially flexible optical networking," *Optical Switching and Networking*, vol. 27, pp. 58–78, 2018.

[15] E. Weizsfeld, "Sur le point par lequel la somme des distances de n points donnVes est minimum," *Tohoku Mathematical Journal, First Series*, vol. 43, pp. 355–386, 1937.

[16] Advanced Energy Industries, Inc, "Powering 5G Radio Access Networks (RAN)." [Online]. Available: https://www.advancedenergy.com/getmedia/6e7cac4c-90b8-4083-bd91-5b57966102a2/en-ep-5g-white-paper_final_1624952677_WP.pdf, 2021.